Supporting Information for

Exploring the Way to Approach the Efficiency Limit of Perovskite Solar Cells by Drift-Diffusion Model

Xingang Ren, Zishuai Wang, Wei E. I. Sha*, Wallace C. H. Choy*

Department of Electrical and Electronic Engineering, The University of Hong Kong, Pokfulam Road, Hong Kong, China.

E-mail: chchoy@eee.hku.hk (W.C.H. Choy), wsha@eee.hku.hk (W. E.I. Sha)

Table S1. The physical parameters used in the drift-diffusion model.

Name	Symbol	Numerical Value
Bandgap	E_g	1.5 eV [1]
Conduction/Valence band	E_C/E_V	-3.9/-5.4eV [1]
Electron and hole mobility	μ_n, μ_p	10 cm^{-3} s^{-1} [2-4]
Density of state of conduction and valence band	N_C, N_V	10^{21} cm^{-3} [4, 5]
Thickness of photon active layer	L	200 nm
Photon generation	G	8×10^{21} cm^{-3} s^{-1}
Radiative recombination limit	R_0^{rad} (=G_0^{dark})	1.07×10^{6} cm^{-3} s^{-1}
Dielectric constant	ε_r	10 [4, 5]
Room temperature thermal energy	k_BT	25.7 meV
Maximum emission angle	θ_m	90^o
Capture coefficient for electrons at trap states	C_n	10^{-8} cm^3 s^{-1} [6]
Capture coefficient for holes at trap states	C_p	10^{-5} cm^3 s^{-1} [6]
Density of trap states	N_t	10^{15}~10^{17} cm^{-3} [6, 7]
Energy level of trap sites	E_t	0.05, 0.10, 0.15 eV

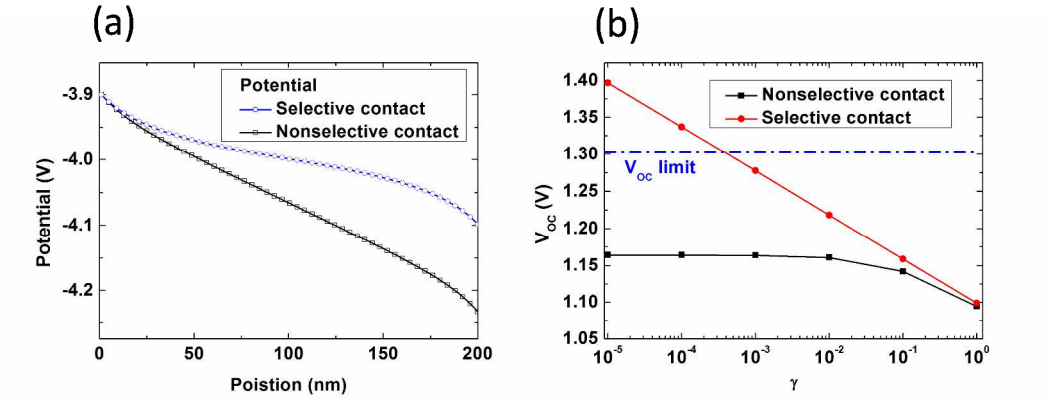

Figure S1. (a) Electrical potential in the PVSCs with the selective and nonselective contacts, respectively. (b) V_{OC} of the PVSCs with the selective and nonselective contacts using different reduction factor γ. The dash-dot line represents the V_{OC} limit (from Table 1).

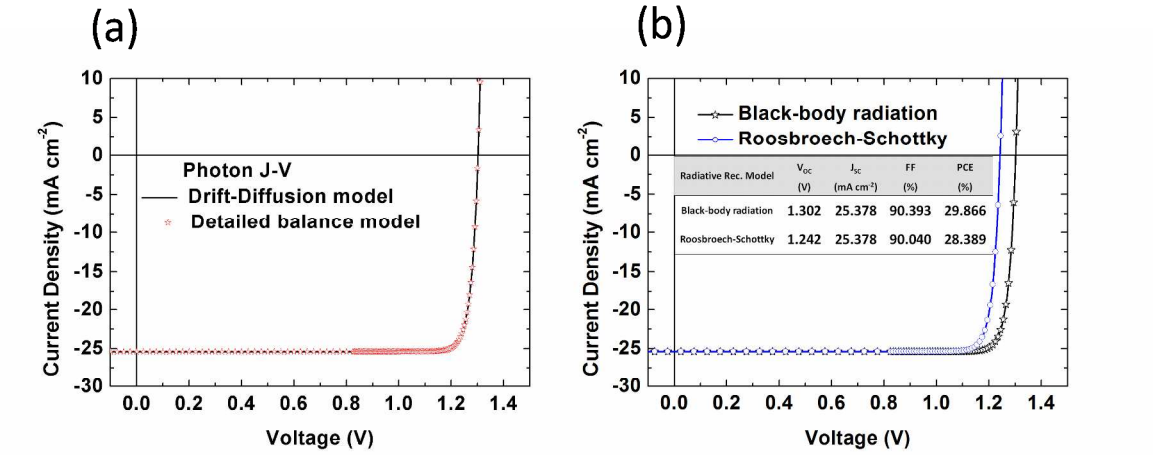

Figure S2. The *J-V* characteristics of PVSCs. (a) Comparisons of *J-V* curves under the light illumination (denoted as photon *J-V*) obtained by the drift-diffusion and detailed balance model, respectively. (b) Comparisons of *J-V* characteristics with the radiative recombination determined by the black-body radiation (Eq. 8) and the Roosbroech-Schottky expression (Eq. 3), respectively. The inset is the corresponding *J-V* characteristics of PVSCs.

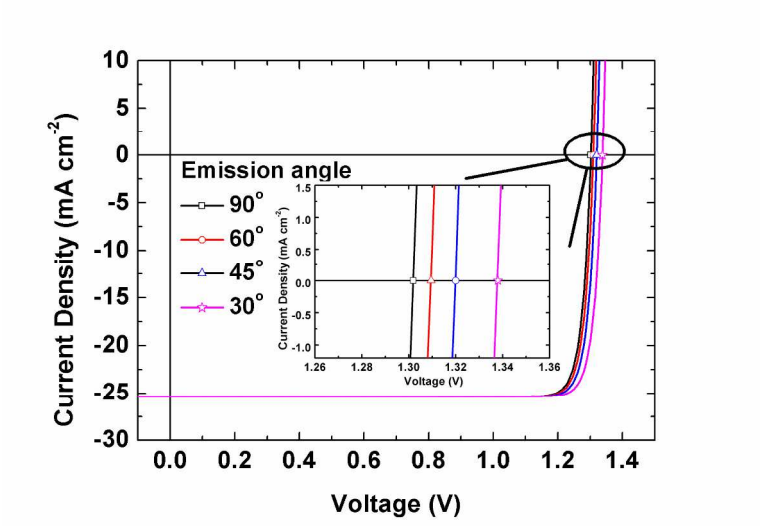

Figure S3. The *J-V* characteristics of PVSCs with different emission angles. The PVSCs under investigation is with selective contact and there is no trap-assisted non-radiative (SRH) recombination in the perovskite. The decrease of the emission angle from 90° to 30° would increase the V_{OC} from 1.30 to 1.34 V, which is mainly due to the reduction of the radiative recombination. It should be noted that the correlation between the restricted emission angle and V_{OC} will become less significant if the SRH recombination is dominant as compared to the radiative recombination.

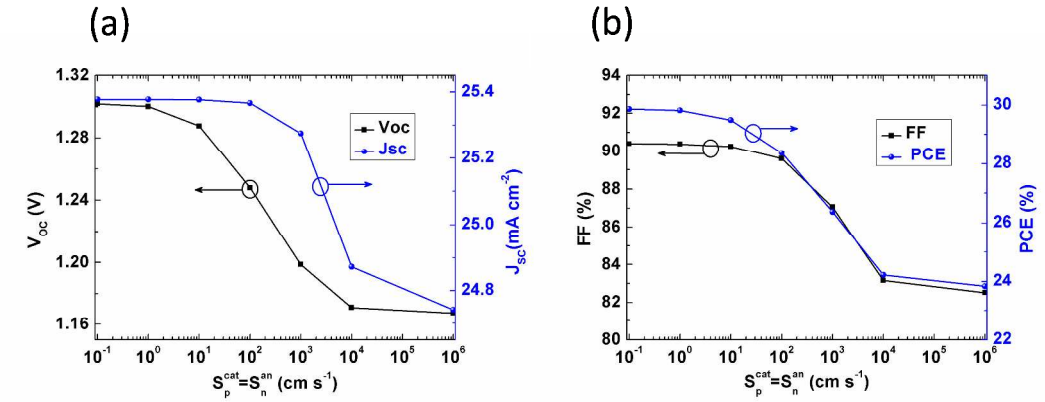

Figure S4. The electrical characteristics of the PVSCs with the nonselective contacts and different surface recombination velocities (S_p^{cat} =S_n^{an} and S_p^{an} =S_n^{cat}=∞). (a) V_{OC} and J_{SC}, (b) FF and PCE.

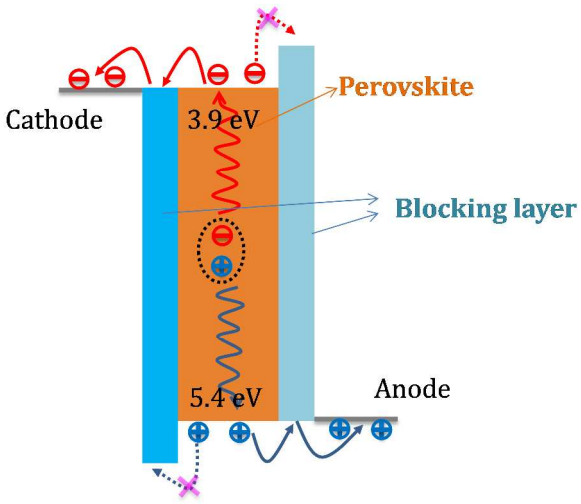

Figure S5. Schematic illustration of perovskite solar cells with the blocking layers. The blocking layers are inserted in between active layer and electrodes for eliminating the minority carrier recombination. The thickness of the blocking layers adopted in the simulation is 10 nm. For simplicity, mobility and dielectric constant of the blocking layer are set as the same as perovskite materials.

Table S2. The summary of PVSC performances with the different trap density N_t and trap energy level E_t.

Trap density N_t (10^{15}cm^{-3})		V_{OC} (V)	J_{SC} (mA cm^{-2})	FF (%)	PCE (%)
E_t=0.05 eV	100	1.23	25.38	89.61	27.89
	10	1.28	25.38	90.16	29.20
	1	1.30	25.38	90.35	**29.76**
E_t =0.1 eV	100	1.18	25.37	88.45	26.51
	10	1.24	25.38	89.67	28.22
	1	1.29	25.38	90.11	**29.40**
E_t =0.15 eV	100	1.14	25.34	85.36	24.58
	10	1.20	25.37	88.71	26.98

1	1.26	25.38	89.43	**28.58**
0*	1.30	25.38	90.39	29.87

*N_t=0 cm^{-3} represents the recombination only includes the bulk radiative recombination.

Regarding the variability/uncertainty of the physical parameter values of $CH_3NH_3PbI_3$ perovskite, we have conducted several simulations to demonstrate the variations of the device performance under the uncertainty of band gap (E_g), density of state (N_C=N_V), carrier mobility (μ_n=μ_p) and permittivity (ε_r), respectively.

Table S3. The summary of device performance with the varied values of the physical parameters for $CH_3NH_3PbI_3$ perovskite. The simulated solar cells are with the selective contact and no defect (i.e. for predicting the PVSC efficiency limit). The physical parameters of the control $CH_3NH_3PbI_3$ perovskite used in manuscript are E_g =1.5 eV, N_C=N_V =10^{21} cm^{-3}, μ_n= μ_p =10 and ε_r =10.

Selective contact +Defect free	V_{OC} (V)	J_{SC} (mA cm^{-2})	FF (%)	PCE (%)
Control	**1.30**	**25.38**	**90.39**	**29.87**
E_g+0.05eV	1.30	25.38	90.39	29.87
N_C(=N_V)×10	1.30	25.38	90.40	29.87
N_C(=N_V)×0.1	1.30	25.38	90.39	29.87
μ_n(=μ_p)×10	1.30	25.38	90.39	29.87
μ_n(=μ_p)×0.1	1.30	25.38	90.39	29.87
ε_r×10	1.30	25.38	90.39	29.87
ε_r×0.1	1.30	25.38	90.28	29.83

In this case, the device configurations are suitable for the prediction of efficiency limit because there is no extrinsic loss in device modeling. In principle, the solar cell performance is only limited by the value of the radiative recombination in this device configuration. In our simulations, the variations of the physical parameters reveal no clear influence on the device performance. Therefore, the prediction capability of the advanced

drift-diffusion model is very robust even there are some uncertainties of the physical parameters value (e.g. bandgap, mobility, density of state and permittivity) for $CH_3NH_3PbI_3$ perovskite.

Reference

1. Abu Laban, W.; Etgar, L. Depleted hole conductor-free lead halide iodide heterojunction solar cells. *Energy Environ. Sci.* **2013**, 6, 3249-3253.
2. Leijtens, T.; Stranks, S. D.; Eperon, G. E.; Lindblad, R.; Johansson, E. M. J.; McPherson, I. J.; Rensmo, H.; Ball, J. M.; Lee, M. M.; Snaith, H. J. Electronic Properties of Meso-Superstructured and Planar Organometal Halide Perovskite Films: Charge Trapping, Photodoping, and Carrier Mobility. *ACS Nano* **2014**, 8, 7147-7155.
3. Wehrenfennig, C.; Eperon, G. E.; Johnston, M. B.; Snaith, H. J.; Herz, L. M. High Charge Carrier Mobilities and Lifetimes in Organolead Trihalide Perovskites. *Adv. Mater.* **2014**, 26, 1584-1589.
4. Yang, W. C.; Yao, Y.; Wu, C. Q. Mechanism of charge recombination in meso-structured organic-inorganic hybrid perovskite solar cells: A macroscopic perspective. *J. Appl. Phys.* **2015**, 117, 155504.
5. Yang, W. C.; Yao, Y.; Wu, C. Q. Origin of the high open circuit voltage in planar heterojunction perovskite solar cells: Role of the reduced bimolecular recombination. *J. Appl. Phys.* **2015**, 117, 095502.
6. Do Kim, H.; Ohkita, H.; Benten, H.; Ito, S. Photovoltaic Performance of Perovskite Solar Cells with Different Grain Sizes. *Adv. Mater.* **2016**, 28, 917-922.
7. Herz, L. M. Charge-Carrier Dynamics in Organic-Inorganic Metal Halide Perovskites. *Annu. Rev. Phys. Chem.* **2016**, 67, 65-89.